



Flooding-related increases in CO₂ and N₂O emissions from a temperate coastal grassland ecosystem

Amanuel W. Gebremichael^{1,2}, Bruce Osborne^{1,2}, Patrick Orr¹

¹UCD School of Earth Sciences, University College Dublin, Belfield, Dublin 4, Ireland

²UCD School of Biology and Environmental Sciences, University College Dublin, Belfield, Dublin 4, Ireland

Correspondence to: Amanuel W. Gebremichael (amanuel.gebremichael@ucdconnect.ie)

Abstract

Given their increasing trend in Europe, an understanding of the role that flooding events play in carbon and nitrogen cycling and greenhouse gas (GHG) emissions will be important for improved assessments of local and regional GHG budgets. This study presents the results of an analysis of the CO₂ and N₂O fluxes from a coastal grassland ecosystem affected by episodic flooding that was of either a relatively short or long duration (SFS and LFS sites, respectively). Compared to the SFS, the annual CO₂ and N₂O emissions were 1.4 and 1.3 times higher at the LFS, respectively. Mean CO₂ emissions during the period of standing water were 144 ± 18.18 and 111 ± 9.51 mg CO₂-C m⁻² h⁻¹, respectively, for the LFS and SFS sites. During the growing season, when there was no standing water, the CO₂ emissions were significantly larger from the LFS (244 ± 24.88 mg CO₂-C m⁻² h⁻¹) than the SFS (183 ± 14.90 mg CO₂-C m⁻² h⁻¹). Fluxes of N₂O ranged from -0.37 to 0.65 mg N₂O-N m⁻² h⁻¹ at the LFS and from -0.50 to 0.55 mg N₂O-N m⁻² h⁻¹ at the SFS, with the larger emissions associated with the presence of standing water at the LFS and during the growing season at the SFS. Overall, soil temperature and moisture content were identified as the main drivers of the seasonal changes in CO₂ fluxes, but neither adequately explained the variations in N₂O fluxes. Analysis of total Carbon (C), Nitrogen (N), microbial biomass and Q₁₀ values, indicated that the higher CO₂ emissions from the LFS were linked to the flooding-associated influx of nutrients and alterations in soil microbial populations. These results demonstrate that annual CO₂ and N₂O emissions can be higher in longer-term flooded sites that receive significant amounts of nutrients and where diffusional limitations due to the presence of standing water is limited to periods of the year when the temperatures are lowest.



1 Introduction

The frequency of flooding events has increased in Europe in the last three decades, and is likely to increase further in a warmer climate, as a consequence of climate change (Beniston et al., 2007; Christensen and Christensen, 2007). Although flooding could have significant implications for greenhouse gas (GHG) emissions 5 due to the effects of a water barrier on gaseous diffusion, as well as through alterations in soil biological and physio-chemical processes (Hansen et al., 2013; Peralta et al., 2013), this has rarely been assessed. It is therefore unclear how flooding influences annual ecosystem GHG budgets, particularly in flood-prone ecosystems that experience variable periods of inundation. The impact of flooding will depend on the timing and duration of the period of inundation, as well as on site-related characteristics related to topography and hydrology. The extent 10 of fresh water flooding will also depend on the frequency and magnitude of rainfall events.

The natural topographic and hydrological conditions of many coastal plain or floodplain wetlands increases the possibility of these ecosystems being rapidly inundated with freshwater following extreme precipitation events or extended periods of rainfall. Episodic flooding is a common feature of these ecosystems, with potential sources of water from inland or inshore incursions, although inundation from freshwater sources is probably 15 more common (Doornkamp, 1998). Many assessments of GHG emissions, and an understanding of the factors that control them, are based on information from ecosystems less prone to flooding episodes. This data may not be directly applicable to coastal areas or floodplains where both the volumes involved and the frequency and duration of water incursions can be high. It is well known that soil water availability can affect the emissions of CO₂ and N₂O by influencing the rates of C and N mineralization (Alongi et al., 1999; Noe et al., 2013) but less 20 clear how variations in standing water levels influence these processes, although this is likely to depend on the extent and the duration of inundation (Lewis et al., 2014). The literature available provides contrasting evidence as to whether soil inundation enhances or impedes organic matter mineralization. Wilson et al., (2011), and Kim et al., (2015) showed the rate of organic matter mineralization can be enhanced after a short hydroperiod (the period the soil area was waterlogged), whereas longer inundation periods suppressed decomposition by limiting 25 oxygen supply (Lewis et al., 2014). Flooding generally promotes anaerobic conditions by excluding air from the pore spaces in the soil that would reduce the mineralisation of organic matter (Altar and Mitsch, 2008). Despite lower mineralisation rates, under these conditions, CO₂ emissions still remain possible from anoxic soils (Glatzel et al., 2004). A number of factors, such as the quality and quantity of substrates available for microbial processes, temperature, soil microbial activity, and oxidation-reduction potential, could impact on the magnitude 30 of CO₂ or N₂O exchange both in flooded and non-flooded ecosystems. High soil organic matter concentrations, in combination with warmer conditions in flooded soil, can also enhance CO₂ production (Oelbermann and Schiff, 2008; Kim et al., 2015). When associated with sufficient oxygen, CO₂ emissions in wetlands increase as a result of accelerated organic matter decomposition, whilst CH₄ production decreases because of aerobic methane oxidation (Smith et al., 2003). Whilst CH₄ is often considered to be a much more significant GHG in 35 permanently wet or flooded ecosystems, this may not be the case where there are only temporary hydroperiods (Audet et al., 2013; Batson et al., 2015), where CO₂ fluxes are still likely to dominate the annual budget. In addition, the effect of temporary or contrasting hydroperiods on N₂O fluxes has received little, if any, consideration. For this reason, we focussed on these two GHGs, which are regarded as the more important ones in many terrestrial ecosystems.



Denitrification and nitrification are often considered as the main mechanisms by which N_2O is produced in soil; although there is evidence that denitrification may be the dominant process for the release of N_2O both under aerobic and anaerobic soil conditions (Bateman and Baggs, 2005). Whilst denitrification and increased N_2O production is enhanced by high soil water contents (Machefer and Díez, 2004; Maag and Vinther, 1996), the
5 frequency and duration of flooding may also be contributory factors controlling the evolution of N_2O . In riparian systems, a shorter flooding duration produced the highest N_2O emissions, which diminished the longer the period of inundation (Jacinthe et al., 2012). In addition to water availability, temperature is also an important variable in determining the production and consumption of N_2O and CO_2 , by affecting the metabolic activity of microorganisms and plants (Davidson and Janssens, 2006; Butterbach-Bahl et al., 2013; Kirwan et al., 2014;
10 Kim et al., 2015).

Flooding stimulates changes in the structure of soil microbial communities (Bossio and Scow, 1998; Unger et al., 2009; Wilson et al., 2011), and this, in turn, affects the rate of decomposition of organic material (Van Der Heijden et al., 2008). The extent of any change in microbial biomass and/or microbial populations could also vary with flooding duration (Rinklebe and Langer, 2006). For example, Wilson et al., (2011) showed significant
15 changes in microbial structure and increases in soil enzymatic activity after the short-term (24 days) inundation of floodplain soil. Nevertheless, an increase in microbial activity and GHG emissions even after short-term flooding is not commonly accepted (Unger et al., 2009; Jacinthe, 2015), and the timing as well as the frequency of flooding events may be important in determining both the microbial community change and the associated GHG emissions. Organic substrate availability (through the breakdown of plant litter or organic compounds
20 transported by flowing water) is considered a key driving factor regulating the activities of soil microorganisms and the mineralization and immobilization of carbon and nitrogen (Badiou et al., 2011; Li et al., 2015). The availability of organic substrates influences the activity of carbon-cycling extracellular enzymes and, as a result, can impact on the rate of CO_2 emissions and potentially other GHGs (Li et al., 2015).

Owing to the episodic nature of flooding events, capturing their impact on GHG emissions is quite challenging
25 and this could perhaps be the reason for the lack of data from field studies. Given the projected increase in flooding events, an evaluation of their impact on GHG emissions is clearly required. Identification of sites with flooding potential before flooding events, and the establishment of the appropriate measurement protocols are crucial steps required to capture the dynamics of GHG fluxes in response to real flooding events. This would enable the capture of the full pattern of GHG fluxes prior to, during and after a flooding event. In this paper, we
30 assess the impact of freshwater inundation, with different hydroperiods, on CO_2 and N_2O fluxes before, during and after real flooding events in a coastal grassland ecosystem over ~2 years. The main objective was to assess the effects of short- and long-term flooding on the dynamics of CO_2 and N_2O fluxes and how this impacts on the annual budgets for each gas. We also evaluate the significance of a number of soil physical, chemical and biological parameters, which may influence the fluxes of CO_2 and N_2O .



2 Materials and methods

2.1 Site description

The study site ($53^{\circ}05'87''$ N, $6^{\circ}04'07''$ W) was situated on a low lying area (~ 0 m a.s.l) of coastal grassland that forms part of the East Coast Nature Reserve (ECNR), a portion of the larger coastal wetland complex called 5 the Murrough wetlands on the east coast of Ireland, near Newcastle, Co. Wicklow (Fig. 1). The site is owned and managed by BirdWatch Ireland, predominantly as a habitat for a wide variety of birds. The grassland area lies between a long drainage ditch that runs in a north-south direction and a shingle beach bordering the Irish Sea. In the past 12 years, restoration methods, including water management, low intensity grazing and crop 10 planting, have been undertaken to maintain the site. The standing water level varies spatially across the site and fluctuates seasonally in response to rainfall and the water-retaining capacity of the drainage ditch. The site experiences near to complete saturation with localised flooding in autumn and winter, but drains and dries out in spring and summer. Despite being located in a coastal area, the ditch water is generally characterized as being fresh water with most sourced from the landward side.

Differences in elevation (~20-25 cm vertical height) over the site result in variations in hydrological 15 connectivity between different portions of the grassland and the ditch water system. Initial monitoring of the general area indicated that this resulted in spatial hydroperiodic differences. The site was therefore divided into two areas based on these hydroperiod characteristics. The site on the more elevated ground is characterized by less frequent and shorter term flooding (SFS) whilst the site located at lower elevations becomes inundated seasonally for an extended period during the winter (longer term flooding: LFS). The plant community of the 20 SFS is mainly dominated by Creeping Bent (*Agrostis stolonifera*) (48%), Velvet grass (*Holcus lanatus*) (27%), Hair grass (*Eleocharis acicularis*) (11%), Meadow grass (*Poa*) (10%) and Couch grass (*Elymus repens*) (7%). The LFS is dominated by grasses and rushes, including Common Couch Grass (*Elytrigia repens*) (80%), Sharp-flowered rush (*Juncus acutiflorus*) (12%) and Curled Dock (*Rumex crispus*) (4%). The mean annual rainfall of 25 the study area is 756 mm (based on data from the Dublin Airport station, 50 km north of our study site, data source: Met Éireann).

2.2 Greenhouse gas measurements

The fluxes of the greenhouse gases, CO_2 and N_2O , were measured using closed chambers. The chambers were made from 16 cm diameter acrylic tube cut to a length of 23 cm with a flat cap of similar material fitted over the top, with an open base. In order to increase the opacity and reflectivity of the Chambers, they were painted dark 30 grey inside and outside and, additionally, their outer surfaces were wrapped in silver duct tape. The chambers were placed on top of collars (~16 cm diameter), with rubber lips around the top, which were inserted into the soil to 5 cm depth. The purpose of the rubber lip was to create a secure seal between the chamber and the collar during the measurements. After establishment of the LFS and SFS sites in September 2013, 6 collars were installed at each site. Individual collars were approximately 6 m apart and the array staggered along two parallel 35 transects. There was ~ 12 m buffer zone between the two sites. During the period when the sites were inundated, the same chamber was used for sampling, but was inserted into a Styrofoam support enabling it to be balanced on top of the collar by floating on the water surface. The collars were also extended to a height of 20 cm by



fitting another similar 15 cm long tube just before the onset of the flooding period. To prevent the chamber from being displaced by any wind during sampling, four thin rods were fixed into the ground around each sampling point to maintain the chamber in position. Sampling of gases was generally undertaken two to four times each month, but less frequently in the winter months.

5 Measurements of the CO₂ and N₂O concentration inside the chamber were made using a Photoacoustic gas analyser (PAS) (Innova 1412, Denmark), connected to the chamber using Teflon tubing. The tubes were 6 m long with a 4 mm inner diameter and the inlet and outlet of the PAS connected to two ports on the top of the chamber. For sampling, the chamber was placed over the collar for between 5 and 6 minutes during which time the gas concentration was analysed 5 to 7 times to complete one sample. Fluxes of CO₂ and N₂O (mg m⁻²hr⁻¹)

10 were calculated using:

$$F = (\Delta C / \Delta t) (V/A)$$

Where $\Delta C / \Delta t$: the rate of change in gas concentration inside the chamber during the chamber placement period, which was calculated by fitting a best fit linear regression line to this data versus time; V : chamber volume ($4.069 \times 10^{-3} \text{ m}^3$); and A : area bounded by the chamber (0.016 m^2). Fluxes of CO₂ and N₂O were computed if

15 linear regressions produced $r^2 > 0.90$ ($P < 0.05$) for CO₂ and $r^2 > 0.70$ ($P < 0.05$) for N₂O.

Annual CO₂ and N₂O emissions for Feb. 2014-Feb. 2015 and May, 2014-April, 2015 were computed by linear interpolation of fluxes for each sampling date. The area under the curve was calculated using the trapezoid rule by integrating the area for 12 month periods. To estimate and compare the contribution of CO₂ and N₂O fluxes to the Global warming potential (GWP), N₂O was converted to CO₂-equivalents by multiplying it by 298

20 (Solomon et al., 2007).

Values of Q₁₀ for CO₂ emissions were computed for the SFS and LFS using the equation $Q_{10} = \exp(\text{slope} \times 10)$, where the slope was derived from the regression coefficient of the exponential equation fitted to the CO₂ flux and temperature data.

2.3 Environmental measurements

25 Along with the flux measurements, other environmental variables that could potentially influence the GHG fluxes were also measured. A weather station, located about ~ 100m from the locality where measurements were made, comprised sensors for air temperature (RHT3nl-CA), humidity (RHT3nl-CA), solar radiation (PYRPA-03) and rainfall (RG2+WS-CA). Average air temperature and cumulative rainfall were recorded at 2 m height every 5, and 60 minutes, respectively. Soil moisture content and temperature were measured adjacent to

30 the collars/chambers using a hand-held Theta probe (Delta-T Devices Ltd., Cambridge, UK) each time gas sampling was performed. The depth of standing water (WD) was measured adjacent to the gas sampling points using a graduated wooden ruler. Redox potential was measured from each collar using a portable Hanna redox meter (HI9125, Hanna Instruments) with a 10 cm redox electrode. Redox potential was measured from the soil surface except when the LFS was flooded above a height of 10 cm, in which case the measurements were



acquired from the surface of water. Complete insertion of the electrode to the top soil was avoided to prevent the uncertain impact of the intrusion of water into the electrode through the rim at the top during sampling.

2.4 Soil sampling for physical and chemical analysis

Sampling of soil from the two sites (each $n = 6$) for analysis of its physicochemical properties was carried out in 5 July 2015 and the samples were then air dried and sieved (2 mm) before analysis. Soil texture was measured using the pipette method (Gee and Bauder, 1986) by first removing the organic content using hydrogen peroxide and then dispersing the samples with sodium hexametaphosphate. Particles were classified as sand (0.063-2 mm), silt (0.002-0.063 mm) and clay (<0.002 mm). Bulk density at the topsoil was determined by drying each 10 soil sample in a soil corer (each 5 cm diameter x 7 cm height) at 105 °C for 48 hrs. The density was calculated by dividing the dried soil mass by the core volume. Soil pH was determined on 10 g soil dispersed in 20 ml of deionized water; after 10 min equilibration, a reading was taken using a pH probe/meter (Thermo Fisher Scientific Inc., Waltham, Michigan, USA) while stirring the suspension. Total Carbon (TC) and Nitrogen (TN) were determined through combustion of finely ground (0.105 mm sieve size) soil using a LECO TruSpec Carbon-Nitrogen analyser (TruSpec®, LECO Corporation, Michigan, USA). Analysis of TC, TN and pH were 15 performed for samples taken every 5 cm from a 25 cm profile (5 samples per sampling point).

Sampling for analysis of $\text{NO}_3\text{-N}$ and $\text{NH}_4\text{-N}$ ($n = 4\text{-}6$ from each of the LFS and SFS site) was carried out on six occasions from 5 cm depths and an extraction performed by mixing 10 g fresh soil with 2 M KCl. After shaking for 1 hour, the KCl extracts were filtered and stored in the freezer until analysis. $\text{NO}_3\text{-N}$ and $\text{NH}_4\text{-N}$ were determined from the extracts using an ion analyser (Lachat, QuikChem®, 5600 Lindburgh Drive, Loveland, 20 Colorado, USA)

2.5 Microbial biomass

Microbial biomass C (MBC) and N (MBN) was determined using the chloroform fumigation extraction method (Vance et al., 1987). 10 g samples of fresh soil ($n=4\text{-}6$) from each site were fumigated in a desiccator with 20 ml ethanol-free chloroform for 72 hours and then extracted with 0.5 M K_2SO_4 . Identical numbers of subsamples 25 were extracted with the same solution but without fumigation the day after sampling. Supernatants from both fumigated and non-fumigated samples were filtered through Whatman No. 1 filter paper and stored in the freezer until analysis. Organic carbon and total nitrogen in the filtrate were analysed using a TOC/TN analyser (Shimadzu, Japan). Estimates of MBC and MBN were derived by calculating the difference between the results of the corresponding fumigated and non-fumigated analysis, divided by the extraction efficiency factor. Factors 30 of 0.45 (Vance et al., 1987) and 0.54 (Brookes et al., 1985) were used for MBC and MBN, respectively, to account for uncompleted extraction of C and N in the microbial cell walls (Jonasson et al., 1996).

2.6 Microbial Activity

Soil enzyme/microbial activities were measured from samples ($n = 4\text{-}6$ per site) collected on six sampling occasions (March, August and October, 2014, March, May and July, 2015). All soil samples were sieved 35 through a 2 mm sieve and analysed in triplicate.



Beta-glucosidase (BG) was determined using the method described by Eivazi and Tabatabai, (1988). After placing 1 g of soil in a 50 ml flask, 0.25 ml toluene, 4 ml of modified universal buffer (pH 6.0) and 1 ml β -D-glucoside and p-nitrophenyl- α solutions (PNG) were added sequentially and mixed by swirling. Samples were then incubated at 37 °C for 1 hr, following which 1 ml of 0.5 M CaCl_2 and 4 ml of 0.1 M tris (hydroxymethyl) aminomethane (pH 12) were added to halt further reactions. The supernatants were filtered and the absorbance of the filtrate measured at 410 nm using a spectrophotometer (Beckman Coulter, DU 530, UV/vis spectrophotometer). For control samples, the same procedure was followed except that PNG was added just before filtering the soil suspension instead of adding it at the beginning.

5 Protease activity (PRO) was determined as described by Kandeler et al., (1999). After 5 ml of sodium caseinate solution was added to 1 g soil, the samples were incubated at 50 °C for 2 hours and then filtered after adding 5 ml of trichloroacetic acid solution. Alkali and Folin-Ciocalteu's reagents were added to the filtrates before protease activity was determined colorimetrically at 700 nm.

10 To determine nitrate reductase activity (NR), 4 ml of 2, 4-Dinitrophenol solution and 1 ml of KNO_3 were added to 5 g samples of soil. After incubation at 25 °C for 24 hours, 10 ml 4 M KCl was added and filtered. To 5 ml of 15 the filtrate, NH_4Cl buffer (pH 8.5) sulphamidamide reagent was added, and the activity of the enzyme nitrate reductase was measured colorimetrically at 520 nm.

15 Total microbial activity was assayed using fluorescein diacetate (FDA), based on the method described by Schnürer and Rosswall, (1982), and later modified by Green et al. (2006). Sodium phosphate buffer (pH 7.6) and FDA lipase substrate were added to flasks containing 1 g samples of soil and incubated for 3 hours at 37 °C. 20 The fluorescein content in the filtered sample was measured at 490 nm.

2.7 Statistical analysis

All statistical analyses were performed using Minitab 16. All the values reported are means of three to six replicates and standard errors were included when required. To investigate the effects of flooding, we tested for significant differences between the two sites (i.e. LFS and SFS) with different hydroperiods, depending on the 25 state of the sites in terms of water-logging (i.e. during and after inundation) over the study period. This was carried out by applying analysis of variance (ANOVA) for each flux, soil enzymatic activity, TC, TN, mineral N and microbial biomass. Functional relationships between potential environmental drivers and the fluxes of CO_2 and N_2O were performed using linear or exponential regression models. Multiple regression analysis was used to determine the relative contribution of more than one independent environmental driver on CO_2 and N_2O 30 fluxes. Normality and homogeneity of the variance of all the models were checked visually from residual versus fitted plots and, when necessary, either square-root or log transformations applied. Differences were considered statistically significant when $P < 0.05$, unless otherwise mentioned.



3 Results

3.1 Soil Characteristics

The relative proportion of clay is higher at the LFS, but both sites have sandy loam soil textures. Soil pH was higher at the SFS than the LFS, and increased with depth at both sites (Table 1). Porosity at the LFS was greater

5 than at the SFS. The soil C and N concentrations were significantly higher ($P<0.001$) at the LFS site, with the greatest difference in the upper soil layers. At both sites, C and N decreased with soil depth, but more gradually at the SFS (Fig. 2a, b).

3.2 Rainfall, water depth, redox potential and air temperature

Depending on the timing and duration of flooding the following periods could be identified, as indicated on Fig.

10 3. Period A: LFS and SFS flooded; Period B: LFS flooded; Period C: neither flooded; Period D: LFS flooded; Period E: neither flooded. Thus, there was no equivalent during 2014/2015 for the Period A (the SFS was not flooded in 2015).

Air temperature followed the typical seasonal pattern (Fig. 3a) for this latitude with the highest values during the summer months (June-August) and the lowest during the winter months (December-February). The values

15 ranged from a high of 23 °C to a low of -3.9 °C with an average of 7.86 °C over the 2-year study period. Rainfall was very variable over the study period (Fig. 3b) with some of the highest rainfall amounts occurring during the warmer months. However, the numbers of rainfall days were higher in the cooler period. The mean annual rainfall (866 mm) at our site during the study period was considerably above the 30 year value (756 mm) measured at the Dublin Airport station.

20 Standing water was only present at the SFS site for ~one month and only in the winter of 2014 and reached a depth of 5 cm (Fig. 3c). In contrast, standing water was present for ~six months at the LFS site in 2015, and reached a depth of ~25 cm in 2014. Whilst standing water at the LFS site was largely associated with the winter periods, it also extended into the spring and autumn periods in 2014/2015 (Fig. 3c).

25 Variations in soil redox potential were broadly correlated with the periods of standing water, with the lowest values occurring in the LFS site in April, 2014 and March 2015 (Fig. 3d) and reflect the reducing conditions associated with longer periods of inundation. In contrast oxidising conditions were always found at the SFS site and these were consistently higher (more positive) than those found at the LFS site (Fig. 3d). Measurements made on the water column, however, indicated that this was always oxidising and had a low but positive redox potential (Fig. 3d).

30 3.3 Seasonal variations in CO₂ and N₂O fluxes

The results are presented with reference to the periods A-E, which represented the state of the sites in relation to water availability. The CO₂ (Fig. 4a) and N₂O (Fig. 4b) emissions showed a marked seasonal variation with the highest CO₂ values during the summer months (June-September) for both sites, which were correlated with the lowest soil moisture values (Fig. 4c) and the highest temperatures (Fig. 4d). The highest CO₂ emissions were



observed from the LFS site during this period (C, E) in each year (Fig. 4a). However, somewhat higher values were found in 2015, particularly for the SFS site (Fig. 4a). The lowest emissions were observed during the winter months when there were no significant differences ($P=0.768$) between the LFS and SFS sites, even though there was standing water at the LFS site (Fig. 3c).

5 Whilst there were no differences in CO_2 emissions between the LFS and SFS during period A (Fig. 4a), an increase in emissions in period B was observed that correlated with the period of declining water levels (Fig. 3c). Within period C, there was also evidence of decreasing CO_2 emissions (Fig. 4a) at the lowest (<20%) soil moisture levels (Fig. 4c). The initial part of Period C is characterised by low and similar values of CO_2 emissions for each site that are not appreciably different ($P=0.956$) from those of the preceding period B. At the
10 LFS, CO_2 emissions during this period ranged from 16.94 to 498.18 $\text{mg CO}_2\text{-C m}^{-2} \text{hr}^{-1}$, whereas at the SFS, the values ranged from 16.68 to 429 $\text{mg CO}_2\text{-C m}^{-2} \text{hr}^{-1}$, and were, for June-September, 2014, significantly different ($P<0.034$).

15 During period D, the highest CO_2 emissions were recorded in the first month of inundation at both the LFS and SFS and declined in both sites over time. In the second growing period (Period E), CO_2 emissions ranged from 53.32 to 477.26 $\text{mg CO}_2\text{-C m}^{-2} \text{h}^{-1}$ at the LFS and from 55.68 to 343.44 $\text{mg CO}_2\text{-C m}^{-2} \text{h}^{-1}$ at the SFS. The difference between the two sites during part of this period (May-August, 2015) was significant ($P=0.013$).

Estimated values of Q_{10} were 2.49 and 2.08 at the LFS and SFS, respectively.

20 Unlike the CO_2 fluxes, the N_2O emissions generally showed no discernible pattern during the study period (Fig. 4b) and there were no systematic changes over time. No significant differences ($P>0.05$) in N_2O fluxes were observed between the LFS and SFS in any of the 5 periods. In the first wetter periods (Periods A and B combined), N_2O fluxes ranged from -0.210 to 0.319 $\text{mg N}_2\text{O-N m}^{-2} \text{h}^{-1}$ and from -0.503 to 0.364 $\text{mg N}_2\text{O-N m}^{-2} \text{h}^{-1}$ at the LFS and SFS, respectively. In period D, the N_2O fluxes from the LFS showed relatively higher variations over time than from the SFS, with values between -0.203 to 0.695 $\text{mg N}_2\text{O-N m}^{-2} \text{h}^{-1}$ for the LFS and -0.307 to 0.206 $\text{mg N}_2\text{O-N m}^{-2} \text{h}^{-1}$ for the SFS. Higher N_2O fluxes were, however, generally observed from the
25 LFS than from the SFS. In the growing season (Period C), SFS showed consistently higher and more positive N_2O fluxes; the maximum emission recorded (0.651 $\text{mg N}_2\text{O-N m}^{-2} \text{h}^{-1}$) was, however, from the LFS, at the end of July. N_2O fluxes less than zero suggest uptake of N_2O , which was more common at the SFS site.

30 Annual CO_2 emissions were 8.18 and 11.24 $\text{Mg CO}_2\text{-C ha}^{-1} \text{y}^{-1}$ from the SFS and LFS, respectively, with values for the LFS 1.4 times higher than that from the SFS. The annual N_2O emissions were 1.3 times higher from the LFS 7.09 $\text{kg N}_2\text{O-N ha}^{-1} \text{y}^{-1}$ compared to the SFS 5.47 $\text{kg N}_2\text{O-N ha}^{-1} \text{y}^{-1}$. In the year SFS was not flooded (May, 2014-April, 2015), the annual CO_2 and N_2O emissions were 8.76 (SFS) and 11.5 (LFS) $\text{Mg CO}_2\text{-C ha}^{-1} \text{y}^{-1}$, and 3.62 (SFS) and 5.49 (LFS) $\text{kg N}_2\text{O-N ha}^{-1} \text{y}^{-1}$, respectively.

3.4 Relationship between CO_2 and N_2O fluxes and environmental parameters

35 Independent testing of the various environmental variables showed that soil temperature, soil water content, redox potential, and, for the LFS, water depth was significantly correlated with soil CO_2 fluxes. Significant



positive correlations were also found between CO_2 emissions and soil temperature for both SFS ($R^2 = 0.44$, $P < 0.001$) and LFS ($R^2 = 0.56$, $P < 0.001$), with a somewhat greater response at LFS (Fig. 5a). A significant negative linear relationship between soil moisture and CO_2 emission was found at the LFS ($R^2 = 0.52$, $P < 0.001$) and the SFS ($R^2 = 0.54$, $P < 0.001$) (Fig. 5b). Correlations between CO_2 emissions and redox potential were low

5 with R^2 values of 0.25 (LFS) and 0.16 (SFS), respectively, but significant at $P < 0.05$. CO_2 emissions at the LFS were exponentially correlated with water depth ($R^2 = 0.45$, $P < 0.001$) (Fig. 5c). Combinations of soil temperature and soil water content in multiple regression analysis only resulted in a small increase in explanatory power to ~ 58 and 66 % at the SFS and LFS, respectively, but no relative contribution of redox potential was found in this analysis.

10 No significant relationship was observed between soil N_2O fluxes and any of, soil temperature, soil moisture, redox potential or water depth at the LFS. At the SFS, soil N_2O fluxes did correlate positively with soil moisture ($R^2 = 0.13$, $P < 0.01$) and soil temperature ($R^2 = 0.13$, $P < 0.01$), but with a low explanatory power. The N_2O flux was also not correlated with redox potential at the SFS.

3.5 Soil enzymatic/microbial activity

15 While there are some significant differences on different sampling dates for BG, FDA and PRO, overall they were of similar magnitude and showed similar variation at both sites (Fig. 6). For period B, BG activity was significantly lower ($P = 0.017$) at the LFS, however, in the second flooding period (the first D), BG was significantly higher ($P = 0.001$) at the LFS than at the SFS. In the later period, E, FDA activity at the LFS was significantly higher ($P = 0.001$) than at the SFS. In contrast, NR activities were consistently and significantly

20 lower ($P < 0.001$) at the SFS and independent of water status (standing water availability).

3.6 Microbial biomass and soil NO_3^- and NH_4^+

Seasonal variations in microbial biomass (MB) appear to differ between the LFS and SFS (Fig. 7). Total MBC was generally higher at the LFS than at the SFS at each sampling period, but particularly significant ($P < 0.01$) for periods B, late D and early E (Fig. 7a). On only two sampling dates was MBN at the LFS slightly lower than

25 at the SFS; for the remaining dates, higher MBN values were observed at the LFS (Fig. 7b). MBC: MBN ratios were significantly higher ($P < 0.01$) at the LFS during periods of standing water (Fig. 7c).

The concentrations of NH_4^+ and NO_3^- were generally higher at the LFS than at the SFS (Table 2). The highest concentrations of NH_4^+ were generally associated with periods of standing water (LFS; March 2014/2015) or immediately after (SFS; March 2014) the disappearance of standing water (Table 2 and Fig. 3c).

30 4 Discussion

The annual CO_2 emissions were 11.24 - 11.5 and 8.18 - 8.76 Mg $\text{CO}_2\text{-C ha}^{-1}\text{y}^{-1}$ from the LFS and SFS, respectively. Longer term flooding therefore increased, rather than reduced, the annual emissions by approximately 40 % and suggests that any increase in freshwater flooding in response to climate change could result in a significant increase in carbon dioxide emissions from these systems. The annual emissions of CO_2

35 found in this study are in line with those previously reported for floodplain wetlands (10.91 ± 0.54 Mg $\text{CO}_2\text{-C}$



$\text{ha}^{-1}\text{y}^{-1}$) (Batson et al., 2015), coastal plain wetlands ($11.29 \text{ Mg CO}_2\text{-C ha}^{-1}\text{y}^{-1}$) (Morse et al., 2012) and occasionally ($9.7 \text{ Mg CO}_2\text{-C ha}^{-1}\text{y}^{-1}$) or frequently flooded ($13 \text{ Mg CO}_2\text{-C ha}^{-1}\text{y}^{-1}$) riparian forests (Jacinthe, 2015). Our results are in part agreement with other investigations of similar ecosystems that examined the impact of flooding on GHGs (Morse et al., 2012; Jacinthe, 2015; Kim et al., 2015; Marín-Muñiz et al., 2015).

5 Jacinthe (2015) reported that CO_2 fluxes during summer were larger from a riparian forest affected by floods in winter and spring than from a flood protected area. Similarly, Morse et al., (2012) found higher rates of CO_2 emission in the dry period from short and intermittently flooded restored wetland habitats compared to both permanently flooded and unflooded sites.

4.1 Relationships between CO_2 fluxes and water and nutrient availability

10 The overall negative relationship between CO_2 emissions and soil moisture (Fig. 5b) suggests that flooding or high soil water availability through the creation of low oxygen conditions impedes the decomposition processes that lead to CO_2 production. Standing water would also act as an additional constraint on annual emissions by acting as a physical barrier to gaseous diffusion. However, somewhat paradoxically, larger annual CO_2 emissions were associated with the site with the longer flooding period. However, the highest CO_2 emissions
15 and the period when the differences in CO_2 emissions between the two sites were greatest occurred in the summer season after the disappearance of standing water, when the soil was better oxygenated (Fig. 3d). No significant differences in CO_2 fluxes between the LFS and SFS were observed during other parts of the year. Whilst the presence of standing water during the autumn/winter months could constrain CO_2 emissions at the LFS by acting as a gaseous barrier, the similar values found for the SFS for the same period indicates that this is
20 unlikely to have a significant impact on the annual emissions. Reductions in mineralisation caused by low temperatures may be the more significant factor at these times of the year, consistent with the strong correlations between CO_2 emissions and temperature that were observed in this study. Clearly, the specific impact of flooding on annual CO_2 emissions could therefore depend critically on the timing of flooding events.

25 Higher CO_2 emissions were obtained at the LFS during the drier parts of the year, when there were similar values for soil moisture/soil temperature at both sites. This may be related to higher organic matter content and nutrient status and a generally higher microbial biomass. Compared to soils supplied with no or little organic matter/nutrients, soils that have received more organic matter are likely to emit substantially larger amounts of CO_2 (Winton and Richardson, 2015). The availability of organic matter is considered one of the most important factors controlling the production of GHGs in wetlands (Badiou et al., 2011). This is often derived from plant
30 production but can be introduced by incoming flood water. In our study, both the difference in total C and N values between the LFS and SFS sites and, specifically, the rapid decline in these nutrients down through the soil profile indicate these are derived largely from external sources, rather than from *in situ*, plant-related material. Had the carbon been contributed mainly from the plant community, similar or higher carbon contents would have been expected from the SFS. However, based on the above ground dry biomass estimations made
35 during the summer of 2014, these were approximately 6 fold higher at the SFS (35.51 Mg ha^{-1}) compared to the LFS (6.02 Mg ha^{-1}), indicating that the nutrients originated from outside the site and were presumably associated with drainage water. Many studies have reported an increase in the release of CO_2 via soil respiration as a result of the increased input of organic matter, particularly in wetlands (Samaritani et al., 2011; Winton and



Richardson, 2015). The source of the organic matter will be dependent on the hydrological connectivity of the wetland to the upstream land use system in addition to plant litter derived from wetland plants (Hernandez and Mitsch, 2007). Given that the C fluxes observed in this work are determined largely by external nutrient inputs, this adds to the growing body of evidence that biogeochemical processes, including greenhouse gas emissions,

5 in floodplain wetlands are predominantly determined by offsite/catchment-related events (Batson et al., 2015). Whilst the results of our study indicate that the availability of organic matter has the major impact on the total CO₂ emissions, annual (seasonal) variations are related to on-site soil water content and temperature, which presumably impact via their effect on the decomposition of organic matter (Curiel Yuste et al., 2007).

4.2 Dependence of CO₂ fluxes on soil temperature

10 Our results also provide some insights regarding the potential effect of temperature on CO₂ production. A larger proportion of the variability in CO₂ fluxes (Fig. 5a) was explained by temperature at the LFS than at the SFS, although the temperatures were essentially identical at these two closely adjacent sites (Fig. 4d). The greater abundance of soil carbon and nitrogen, accompanied by a generally higher microbial biomass suggests substrate availability at the LFS was greater for soil microbial processes (Wang et al., 2003). The higher Q₁₀ values at the 15 LFS (2.49) compared to the SFS (2.08) also suggest differences in the microbial populations at the two sites. The higher Q₁₀ values for CO₂ emissions at the LFS indicates that longer term flooded sites could be more sensitive to climate change related warming (Zhou et al., 2014).

The subtle effects of temperature on its own are illustrated by the CO₂ fluxes from the LFS in two episodes near the beginning and end of the flooding period (Period B and D) when there was standing water and little variation 20 in soil moisture status (Fig. 4a). Firstly, just before the end of the first flooding period (Period B, terminated April 2014), a decrease in standing water level coincided with an increase in temperature that resulted in a pulse of CO₂ emission. Secondly, a few days after the beginning of the second flooding event (Period D, initiated October, 2014), a CO₂ efflux was observed in conjunction with a temperature increase. In neither case was there 25 a similar response in the SFS. This indicates that temperature can, at some times, have a greater impact than water availability in determining CO₂ fluxes. Whilst the reason(s) for these temperature-associated emissions is not clear, it could be due to release of accumulated air bubbles in the sediment (ebullition) at the LFS (Venkiteswaran et al., 2013). However, due to the higher solubility of CO₂, the contribution of ebullition as a mechanism for CO₂ emissions is often thought to be very low (Abril et al., 2005). In general, most of the higher CO₂ fluxes (>170 mg CO₂-C m⁻² h⁻²) occurred when the soil temperature was above 15 °C with a soil moisture 30 of 20-40 %. Kim et al., (2015) showed an increase in CO₂ production with increasing temperature from incubated flooded and non-flooded boreal soil. This again highlights the importance of the timing of flooding events and also the need to consider temperature variations when investigating the impact of flooding on GHG emissions.

4.3 Effect of redox potential on the soil CO₂ and N₂O fluxes

35 Episodic flooding and draining is the likely cause of the greater seasonal variation in the oxidation-reduction level at the LFS compared to the more limited variation at the SFS where there was only a short hydroperiod. The weak correlation between redox potential and CO₂, and the absence of a relationship with N₂O emissions



(Section 3.4) for the two sites, suggests soil redox potential had minimal influence on the emissions of these gases. This appears to contrast with the finding of Marín-Muñiz et al., (2015), who identified redox potential and water level as the main factors controlling CO₂, N₂O and CH₄ emissions in coastal freshwater wetlands.

The redox potential of the SFS and LFS sites were, however, different and the ranges at which the highest CO₂ emissions occurred were 220-362 mv and 145-259 mv at the SFS and LFS, respectively. The data could imply that the larger CO₂ fluxes were enhanced by more oxidized soil conditions. However, they were not dependent on the redox level of the soil as the highest CO₂ emissions at the LFS occurred in the lower end of the redox range observed. The lower redox potential at the LFS after the disappearance of standing water could be due to the free-draining nature of this site and/or the presence of a higher organic matter content. Gardiner and James, (2012) showed a marked decrease in the redox potential (more negative) as a result of organic matter addition in their wet soil microcosm study. The redox status of soil is also controlled by the availability of electron acceptors and microbial activity (Oktyabrskii and Smirnova, 2012; Hunting and Kampfrahth, 2013).

No particular redox range associated with greater N₂O emissions was confidently identified. The fluxes were somewhat higher when the redox value was above 249 mv at the SFS and between -232 and 228 mv at the LFS. Many previous studies have reported higher N₂O emissions in flood-affected wetlands over a wide range of redox potentials (-100 to 430 mv) (Yu et al., 2001; Włodarczyk et al., 2003; Morse et al., 2012). Marín-Muñiz et al., (2015) found an optimum range of 100-360 mv for reduction of nitrate to N₂O from a coastal wetland, whereas Morse et al., (2012) reported values of 89 and 5.3 mv from rarely and intermittently flooded areas, respectively, as the conditions conducive for N₂O production.

20 **4.4 Relationship between water depth and CO₂ and N₂O fluxes**

Several studies have shown a negative relationship between GHGs and water level in riparian wetlands (e.g. Mander et al., 2015; Marín-Muñiz et al., 2015). Increases in water depth at the LFS during the flooding period were accompanied by a decrease in the rate of CO₂ emissions, perhaps due to a decrease in near-surface oxygen supply as a result of high standing water levels. Water depth has been shown to be more significant than 25 temperature in determining the variation in CO₂ fluxes during the inundation period (Dixon et al., 2014). Multiple regression analysis of CO₂ fluxes showed a significant paraboloid relationship ($R^2 = 0.62$, $P < 0.001$) with water depth and soil temperature combined (Fig. 8) but most of this variation is explained by changes in water depth alone ($R^2 = 0.45$, $P < 0.001$) (Fig. 5c). Peak CO₂ fluxes (above 75 mg CO₂-C m⁻²h⁻²) were recorded during Periods B and D when less than 9 cm water depths were coupled with soil temperatures above 11 °C. No 30 major variations in CO₂ fluxes were observed when the water depths were greater than 12 cm above the soil surface. Even though some studies have shown a significant relationship between N₂O fluxes and water depth (Mander et al., 2015; Marín-Muñiz et al., 2015), no correlation was found in this study (Section 3.4). Audet et al., (2013) also found no significant impact of water depth on N₂O emission from a temperate riparian wetland.

4.5 N₂O fluxes and their controlling factors

35 No relationship was found between N₂O fluxes and soil moisture content or temperature at the LFS and only a weak relationship at the SFS, suggesting the influence of these variables on nitrification and denitrification



processes leading to N_2O production from these sites is limited. Several other environmental factors such as pH, oxygen concentration and nitrogen availability are known to affect the production of N_2O (Ullah and Zinati, 2006; Van den Heuvel et al., 2011; Burgin and Groffman, 2012). In this study, the lower pH, as well as a higher nitrogen availability and higher MBC at the LFS would be expected to favour N_2O emissions (Liu et al., 2010);

5 Van den Heuvel et al., 2011). However, apart from the constantly positive, and higher, N_2O fluxes observed at the LFS for many of the sampling dates in period D, no appreciable differences in N_2O emission were detected between the two sites. The generally higher N_2O emissions from the LFS in period D might be associated with the persistent anaerobic conditions that would have favoured a transient reduction of NO_3^- to N_2O . Higher soil NH_4^+ concentrations under largely anoxic conditions (Periods A, B and D) and its progressive decrease through

10 the aerobic period (Periods C and E) in the two sites (Table 2) indicate increased nitrification and ammonia oxidation that may lead to N_2O production as aeration of soil and gas diffusion improves (Firestone and Davidson, 1989). This is a potential explanation for the larger N_2O emissions observed at the SFS during the larger part of the first, and, in a few occasions, during the second summer period. Continuous and relatively low, or negative, N_2O emissions were observed for both sites during the early part of periods C and E (i.e. after

15 draining of the flood water at the LFS). This may be due to increased N uptake by growing vegetation at the two sites, offsetting any tendency for water drainage to have increased soil aeration and thereby promote N_2O formation. This potentially also explains the absence of N_2O fluxes of a similar magnitude at the LFS during the summer where, unlike at the SFS, the immediate development and recovery of grasses, was likely impeded by the preceding episode of prolonged water-logging (Steffens et al., 2005).

20 The annual N_2O emissions estimated in this work (7.09 and 5.47 kg $\text{N}_2\text{O-N ha}^{-1} \text{y}^{-1}$ in the LFS and SFS, respectively) are within the range of emissions obtained in restored temperate wetlands in Denmark and The Netherlands (Hefting et al., 2003; Audet et al., 2013). Fisher et al., (2014) reported higher annual N_2O emissions (4.32 kg $\text{N}_2\text{O-N ha}^{-1}$) from flood-prone riparian buffer zones in Indiana, USA, compared to unflooded buffer zones (1.03 kg $\text{N}_2\text{O-N ha}^{-1}$).

25 In terms of the contribution of each gas to the global warming potential (GWP), expressed as CO_2 -equivalents, N_2O contributed only 15 to 17 %, to GWP, which is low compared to the CO_2 contribution of 83-85 %. We have not assessed the contribution of CH_4 gaseous emissions, although other findings report a high contribution of methane to the GWP from floodplains and freshwater wetlands (Altor and Mitsch, 2006; Koh et al., 2009). However, this may not always be the case and Jacinthe, (2015) showed that some terrestrial riparian ecosystems,

30 which were exposed to different flooding frequencies, routinely acted as a strong sink for CH_4 , except for a small contribution in emissions from permanently flooded sites.

5 Conclusion

This study provides evidence that the interaction of a grassland ecosystem with the hydrologic regime, impacts on the annual emissions of greenhouse gases. Flooding duration affected the dynamics of CO_2 and, to a lesser extent, N_2O fluxes. Total emissions of CO_2 increased with flooding duration, with longer term (~6 months) flooding associated with higher annual emissions than the shorter term (~2-4 weeks) flooding. Temperature and soil water content are identified as the most important factors controlling the seasonal pattern of the CO_2 fluxes,



especially in the longer term flooded site. The higher emissions from the longer term flooded site is likely linked to the higher inputs of organic materials/nutrients, and associated increases in microbial biomass and possibly changes in the microbial populations. In contrast, no individual environmental parameter, or any combination of them, was found to have a major influence on the emissions of N_2O . However, flooding enhanced N_2O production during the period in which water was standing on the longer term flooded site, likely due to enhanced denitrification, demonstrating the probable influence of inundation on the dynamics of N_2O from coastal freshwater grasslands. The controlling mechanisms underpinning the observed N_2O fluxes are not clear. However, the information obtained from the current study indicates that the contribution of N_2O emissions to global warming would be minimal. A more extensive study of the effect of specific hydrologic patterns (flooding frequency, timing and duration) on the dynamics of GHGs, including CH_4 , would be required to better assess the global warming potential of flood-affected ecosystems.

Acknowledgment

This project is part of the Earth and Natural Sciences Doctoral Studies Programme, which is funded by the Higher Education Authority (HEA) through the Programme for Research at Third Level Institutions, Cycle 5 (PRTLI-5) and is co-funded by the European Regional Development Fund (ERDF). We wish to thank BirdWatch Ireland in Wicklow for providing the study site for this research and their support through the process of site formation.

20

25

30



References

Abril, G., Guérin, F., Richard, S., Delmas, R., Galy-Lacaux, C., Gosse, P., Tremblay, A., Varfalvy, L., Dos Santos, M. A., and Matvienko, B.: Carbon dioxide and methane emissions and the carbon budget of a 10-year old tropical reservoir (Petit Saut, French Guiana), *Global Biogeochemical Cycles*, 19, 3197-3223, 2005.

5 Alongi, D. M., Tirendi, F., Dixon, P., Trott, L. A., and Brunskill, G. J.: Mineralization of Organic Matter in Intertidal Sediments of a Tropical Semi-enclosed Delta, *Estuarine, Coastal and Shelf Science*, 48, 451-467, 1999.

Altor, A. E. and Mitsch, W. J.: Methane flux from created riparian marshes: Relationship to intermittent versus continuous inundation and emergent macrophytes, *Ecological Engineering*, 28, 224-234, 2006.

10 Altor, A. and Mitsch, W.: Pulsing hydrology, methane emissions and carbon dioxide fluxes in created marshes: A 2-year ecosystem study, *Wetlands*, 28, 423-438, 2008.

Audet, J., Elsgaard, L., Kjaergaard, C., Larsen, S. E., and Hoffmann, C. C.: Greenhouse gas emissions from a Danish riparian wetland before and after restoration, *Ecological Engineering*, 57, 170-182, 2013.

15 Badiou, P., McDougal, R., Pennock, D., and Clark, B.: Greenhouse gas emissions and carbon sequestration potential in restored wetlands of the Canadian prairie pothole region, *Wetlands Ecology and Management*, 19, 237-256, 2011.

Bateman, E. J. and Baggs, E. M.: Contributions of nitrification and denitrification to N₂O emissions from soils at different water-filled pore space, *Biol Fertil Soils*, 41, 379-388, 2005.

20 Batson, J., Noe, G. B., Hupp, C. R., Krauss, K. W., Rybicki, N. B., and Schenk, E. R.: Soil greenhouse gas emissions and carbon budgeting in a short-hydroperiod floodplain wetland, *Journal of Geophysical Research: Biogeosciences*, 120, 77-95, 2015.

Beniston, M., Stephenson, D. B., Christensen, O. B., Ferro, C. A. T., Frei, C., Goyette, S., Halsnaes, K., Holt, T., Jylhä, K., Koffi, B., Palutikof, J., Schöll, R., Semmler, T., and Wołt, K.: Future extreme events in European climate: an exploration of regional climate model projections, *Climatic Change*, 81, 71-95, 2007.

25 Bossio, D. A. and Scow, K. M.: Impacts of Carbon and Flooding on Soil Microbial Communities: Phospholipid Fatty Acid Profiles and Substrate Utilization Patterns, *Microb Ecol*, 35, 265-278, 1998.

Brookes, P. C., Landman, A., Pruden, G., and Jenkinson, D.: Chloroform fumigation and the release of soil nitrogen: a rapid direct extraction method to measure microbial biomass nitrogen in soil, *Soil Biology and Biochemistry*, 17, 837-842, 1985.

30 Burgin, A. J. and Groffman, P. M.: Soil O₂ controls denitrification rates and N₂O yield in a riparian wetland, *Journal of Geophysical Research: Biogeosciences*, 117, n/a-n/a, 2012.

Butterbach-Bahl, K., Baggs, E. M., Dannenmann, M., Kiese, R., and Zechmeister-Boltenstern, S.: Nitrous oxide emissions from soils: how well do we understand the processes and their controls?, *Philosophical Transactions of the Royal Society of London B: Biological Sciences*, 368, 2013.

35 Christensen, J. and Christensen, O.: A summary of the PRUDENCE model projections of changes in European



climate by the end of this century, *Climatic Change*, 81, 7-30, 2007.

Curiel Yuste, J., Baldocchi, D., Gershenson, A., Goldstein, A., Misson, L., and Wong, S.: Microbial soil respiration and its dependency on carbon inputs, soil temperature and moisture, *Global Change Biology*, 13, 2018-2035, 2007.

5 Davidson, E. A. and Janssens, I. A.: Temperature sensitivity of soil carbon decomposition and feedbacks to climate change, *Nature*, 440, 165-173, 2006.

Dixon, S. D., Qassim, S. M., Rowson, J. G., Worrall, F., Evans, M. G., Boothroyd, I. M., and Bonn, A.: Restoration effects on water table depths and CO₂ fluxes from climatically marginal blanket bog, *Biogeochemistry*, 118, 159-176, 2014.

10 Doornkamp, J. C.: Coastal flooding, global warming and environmental management, *Journal of Environmental Management*, 52, 327-333, 1998.

Eivazi, F. and Tabatabai, M. A.: Glucosidases and galactosidases in soils, *Soil Biology and Biochemistry*, 20, 601-606, 1988.

Firestone, M. K. and Davidson, E. A.: Microbiological basis of NO and N₂O production and consumption in soil, *Exchange of trace gases between terrestrial ecosystems and the atmosphere*, 47, 7-21, 1989.

15 Fisher, K., Jacinthe, P., Vidon, P., Liu, X., and Baker, M.: Nitrous oxide emission from cropland and adjacent riparian buffers in contrasting hydrogeomorphic settings, *Journal of environmental quality*, 43, 338-348, 2014.

Gardiner, D. T. and James, S.: Wet Soil Redox Chemistry as Affected by Organic Matter and Nitrate, *American Journal of Climate Change*, 1, 205, 2012.

20 Gee, G. W., and J.W. Bauder Particle-size analysis: In: A. Klute (Editor), *Methods of Soil Analysis*. Part 1, 2nd ed., *Agronomy*, 9, 383-399, 1986.

Glatzel, S., Basiliko, N., and Moore, T.: Carbon dioxide and methane production potentials of peats from natural, harvested and restored sites, eastern Québec, Canada, *Wetlands*, 24, 261-267, 2004.

25 Green, V. S., Stott, D. E., and Diack, M.: Assay for fluorescein diacetate hydrolytic activity: Optimization for soil samples, *Soil Biology and Biochemistry*, 38, 693-701, 2006.

Hansen, M., Clough, T. J., and Elberling, B.: Flooding-induced N₂O emission bursts controlled by pH and nitrate in agricultural soils, *Soil Biology and Biochemistry*, 69, 17-24, 2014.

Hefting, M. M., Bobbink, R., and de Caluwe, H.: Nitrous oxide emission and denitrification in chronically nitrate-loaded riparian buffer zones, *Journal of environmental quality*, 32, 1194-1203, 2003.

30 Hernandez, M. E. and Mitsch, W. J.: Denitrification Potential and Organic Matter as Affected by Vegetation Community, Wetland Age, and Plant Introduction in Created Wetlands, *Journal of environmental quality*, 36, 333-342, 2007.

Hunting, E. R. and Kampfraath, A. A.: Contribution of bacteria to redox potential (E h) measurements in sediments, *Int. J. Environ. Sci. Technol.*, 10, 55-62, 2013.



Jacinthe, P., Bills, J., Tedesco, L., and Barr, R.: Nitrous oxide emission from riparian buffers in relation to vegetation and flood frequency, *Journal of environmental quality*, 41, 95-105, 2012.

Jacinthe, P. A.: Carbon dioxide and methane fluxes in variably-flooded riparian forests, *Geoderma*, 241–242, 41-50, 2015.

5 Jonasson, S., Michelsen, A., Schmidt, I. K., Nielsen, E. V., and Callaghan, T. V.: Microbial biomass C, N and P in two arctic soils and responses to addition of NPK fertilizer and sugar: implications for plant nutrient uptake, *Oecologia*, 106, 507-515, 1996.

Kandeler, E., Luxhøi, J., Tscherko, D., and Magid, J.: Xylanase, invertase and protease at the soil–litter interface of a loamy sand, *Soil Biology and Biochemistry*, 31, 1171-1179, 1999.

10 Kim, Y., Ullah, S., Roulet, N. T., and Moore, T. R.: Effect of inundation, oxygen and temperature on carbon mineralization in boreal ecosystems, *Science of The Total Environment*, 511, 381-392, 2015.

Kirwan, M. L., Guntenspergen, G. R., and Langley, J. A.: Temperature sensitivity of organic-matter decay in tidal marshes, *Biogeosciences*, 11, 4801-4808, 2014.

15 Koh, H.-S., Ochs, C. A., and Yu, K.: Hydrologic gradient and vegetation controls on CH₄ and CO₂ fluxes in a spring-fed forested wetland, *Hydrobiologia*, 630, 271-286, 2009.

Lewis, D. B., Brown, J. A., and Jimenez, K. L.: Effects of flooding and warming on soil organic matter mineralization in *Avicennia germinans* mangrove forests and *Juncus roemerianus* salt marshes, *Estuarine, Coastal and Shelf Science*, 139, 11-19, 2014.

20 Li, X., Hou, L., Liu, M., Lin, X., Li, Y., and Li, S.: Primary effects of extracellular enzyme activity and microbial community on carbon and nitrogen mineralization in estuarine and tidal wetlands, *Appl Microbiol Biotechnol*, 99, 2895-2909, 2015.

Liu, B., Mørkved, P. T., Frostegård, Å., and Bakken, L. R.: Denitrification gene pools, transcription and kinetics of NO, N₂O and N₂ production as affected by soil pH, *FEMS Microbiology Ecology*, 72, 407-417, 2010.

25 Maag, M. and Vinther, F. P.: Nitrous oxide emission by nitrification and denitrification in different soil types and at different soil moisture contents and temperatures, *Applied Soil Ecology*, 4, 5-14, 1996.

Machefert, S. E. and Dise, N. B.: Hydrological controls on denitrification in riparian ecosystems, *Hydrol. Earth Syst. Sci.*, 8, 686-694, 2004.

30 Mander, Ü., Maddison, M., Soosaar, K., Teemusk, A., Kanal, A., Uri, V., and Truu, J.: The impact of a pulsing groundwater table on greenhouse gas emissions in riparian grey alder stands, *Environ Sci Pollut Res*, 22, 2360-2371, 2015.

Marín-Muñiz, J. L., Hernández, M. E., and Moreno-Casasola, P.: Greenhouse gas emissions from coastal freshwater wetlands in Veracruz Mexico: Effect of plant community and seasonal dynamics, *Atmospheric Environment*, 107, 107-117, 2015.

35 Morse, J. L., Ardón, M., and Bernhardt, E. S.: Greenhouse gas fluxes in southeastern US coastal plain wetlands under contrasting land uses, *Ecological Applications*, 22, 264-280, 2012.



Noe, G., Hupp, C., and Rybicki, N.: Hydrogeomorphology Influences Soil Nitrogen and Phosphorus Mineralization in Floodplain Wetlands, *Ecosystems*, 16, 75-94, 2013.

Oelbermann, M. and Schiff, S. L.: Quantifying Carbon Dioxide and Methane Emissions and Carbon Dynamics from Flooded Boreal Forest Soil, *Journal of environmental quality*, 37, 2037-2047, 2008.

5 Oktyabrskii, O. N. and Smirnova, G. V.: Redox potential changes in bacterial cultures under stress conditions, *Microbiology*, 81, 131-142, 2012.

Peralta, A. L., Ludmer, S., and Kent, A. D.: Hydrologic history influences microbial community composition and nitrogen cycling under experimental drying/wetting treatments, *Soil Biology and Biochemistry*, 66, 29-37, 2013.

10 Rinklebe, J. and Langer, U.: Microbial diversity in three floodplain soils at the Elbe River (Germany), *Soil Biology and Biochemistry*, 38, 2144-2151, 2006.

Samaritani, E., Shrestha, J., Fournier, B., Frossard, E., Gillet, F., Guenat, C., Niklaus, P., Tockner, K., Mitchell, E., and Luster, J.: Heterogeneity of soil carbon pools and fluxes in a channelized and a restored floodplain section (Thur River, Switzerland), *Hydrology and Earth System Sciences Discussions*, 8, 1059-1091, 2011.

15 Schnürer, J. and Rosswall, T.: Fluorescein diacetate hydrolysis as a measure of total microbial activity in soil and litter, *Applied and environmental microbiology*, 43, 1256-1261, 1982.

Smith, K., Ball, T., Conen, F., Dobbie, K., Massheder, J., and Rey, A.: Exchange of greenhouse gases between soil and atmosphere: interactions of soil physical factors and biological processes, *European Journal of Soil Science*, 54, 779-791, 2003.

20 Solomon, S., Qin, D., Manning, M., Chen, Z., Marquis, M., Averyt, K., Tignor, M., and Miller, H.: IPCC, 2007: summary for policymakers, *Climate change*, 2007. 93-129, 2007.

Steffens, D., Hutsch, B., Eschholz, T., Losak, T., and Schubert, S.: Water logging may inhibit plant growth primarily by nutrient deficiency rather than nutrient toxicity, *Plant Soil and Environment*, 51, 545, 2005.

25 Ullah, S. and Zinati, G.: Denitrification and nitrous oxide emissions from riparian forests soils exposed to prolonged nitrogen runoff, *Biogeochemistry*, 81, 253-267, 2006.

Unger, I. M., Kennedy, A. C., and Muzika, R.-M.: Flooding effects on soil microbial communities, *Applied Soil Ecology*, 42, 1-8, 2009.

Van den Heuvel, R., Bakker, S., Jetten, M., and Hefting, M.: Decreased N₂O reduction by low soil pH causes high N₂O emissions in a riparian ecosystem, *Geobiology*, 9, 294-300, 2011.

30 Van Der Heijden, M. G. A., Bardgett, R. D., and Van Straalen, N. M.: The unseen majority: soil microbes as drivers of plant diversity and productivity in terrestrial ecosystems, *Ecology Letters*, 11, 296-310, 2008.

Vance, E., Brookes, P., and Jenkinson, D.: An extraction method for measuring soil microbial biomass C, *Soil Biology and Biochemistry*, 19, 703-707, 1987.

35 Venkiteswaran, J. J., Schiff, S. L., St. Louis, V. L., Matthews, C. J. D., Boudreau, N. M., Joyce, E. M., Beaty, K. G., and Bodaly, R. A.: Processes affecting greenhouse gas production in experimental boreal reservoirs,



Global Biogeochemical Cycles, 27, 567-577, 2013.

Wang, W. J., Dalal, R. C., Moody, P. W., and Smith, C. J.: Relationships of soil respiration to microbial biomass, substrate availability and clay content, *Soil Biology and Biochemistry*, 35, 273-284, 2003.

5 Wilson, J. S., Baldwin, D. S., Rees, G. N., and Wilson, B. P.: The effects of short-term inundation on carbon dynamics, microbial community structure and microbial activity in floodplain soil, *River Research and Applications*, 27, 213-225, 2011.

Winton, R. S. and Richardson, C.: The Effects of Organic Matter Amendments on Greenhouse Gas Emissions from a Mitigation Wetland in Virginia's Coastal Plain, *Wetlands*, 35, 969-979, 2015.

10 Włodarczyk, T., Stępniewska, Z., and Brzezinska, M.: Denitrification, organic matter and redox potential transformations in Cambisols, *Int. Agrophysics*, 17, 219-227, 2003.

Yu, K., Wang, Z., Vermoesen, A., Patrick Jr, W., and Van Cleemput, O.: Nitrous oxide and methane emissions from different soil suspensions: effect of soil redox status, *Biol Fertil Soils*, 34, 25-30, 2001.

Zhou, W., Hui, D., and Shen, W.: Effects of soil moisture on the temperature sensitivity of soil heterotrophic respiration: a laboratory incubation study, *PLoS ONE*, 9, e92531, 2014.

15

20

25



Tables and Figures

Table 1. Soil properties (0-10 cm) in the LFS and SFS. Values are mean of N=4-6.

Soil properties	LFS	SFS
Sand (%)	64.40	69.00
Clay (%)	16.00	6.50
Bulk density (g cm ⁻³)	0.73	1.02
Porosity	0.73	0.61
pH	4.79	5.28
Total Carbon (g kg ⁻¹)	204.70	120.00
Total Nitrogen (g kg ⁻¹)	38.50	10.70
C to N ratio	5.31	11.21

5

10 Table 2. Soil NH₄⁺ and NO₃⁻ concentrations at 0-5 cm depths (mg N kg⁻¹) for different sampling dates in 2014 and 2015.

Date (Period)	LFS		SFS	
	NH ₄ ⁺	NO ₃ ⁻	NH ₄ ⁺	NO ₃ ⁻
04 March, 2014 (B)	30.49	0.99	25.63	0.52
30 April, 2014 (C)	12.93	0.30	4.37	0
19 August, 2014 (C)	12.47	0.28	16.85	0.29
08 March, 2015 (D)	25.80	0	17.66	0
28 May, 2015 (E)	18.24	2.28	15.88	0.12
17 July, 2015 (E)	13.08	0.51	12.11	0.24

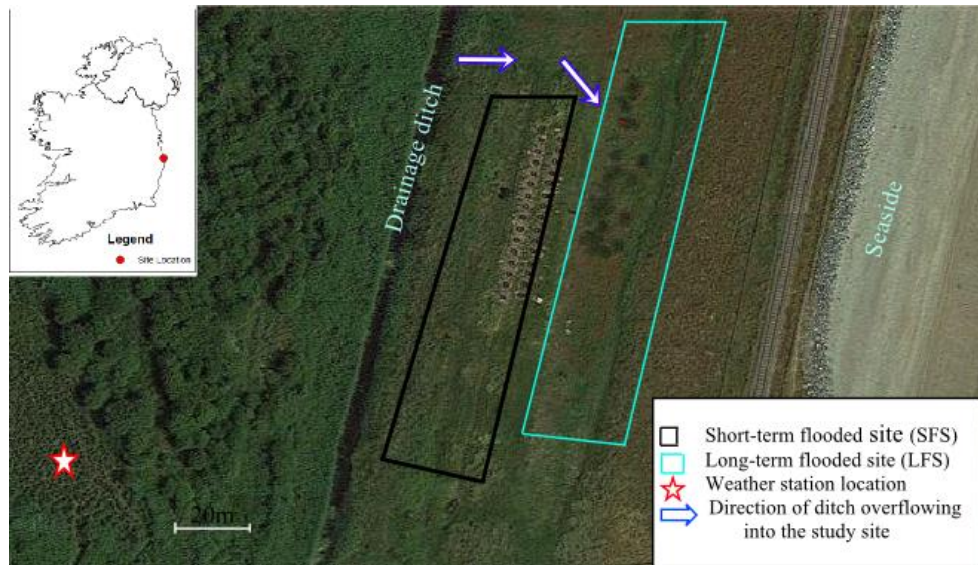
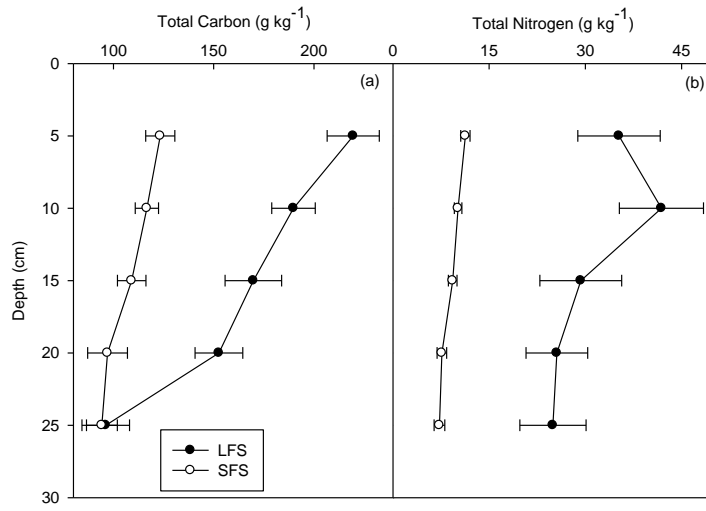


Figure 1 Aerial photograph of part of East Coast Nature Reserve at Blackditch Wood, County Wicklow, showing the study sites and the direction in which water flows during flooding. Inset shows map of Ireland with site location indicated.



5

Figure 2 Profile of (a) total carbon, and (b) total nitrogen in the LFS and SFS. Mean values ($n=6$) are from each level within a profile and the horizontal bars represent the standard errors.

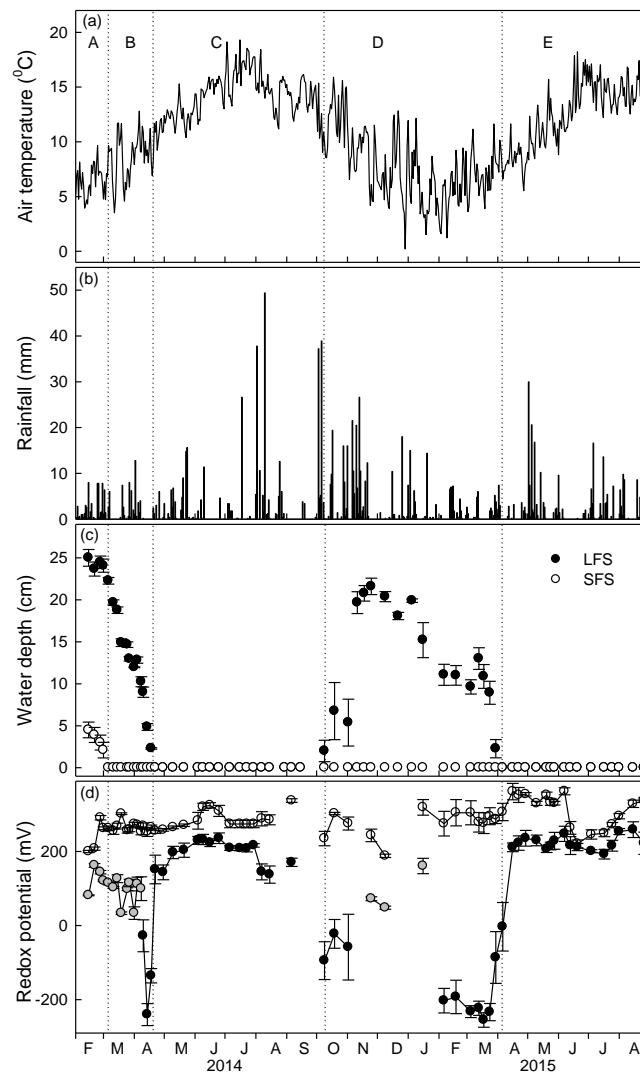


Figure 3 Variations in (a) daily air temperature, (b) daily rainfall, (c) average water depth above the soil surface, and (d) redox potential at the study sites. Open circles represent values redox from the ground surface of the SFS, black filled circles represents values from the soil surface of the LFS and grey filled circles show values from the water surface while LFS was flooded to greater than 10 cm depth. Period A: LFS and SFS flooded; Period B: LFS flooded; Period C: neither flooded; Period D: LFS flooded; Period E: neither flooded. Thus, there was no equivalent of period A during late 2014 – early 2015.

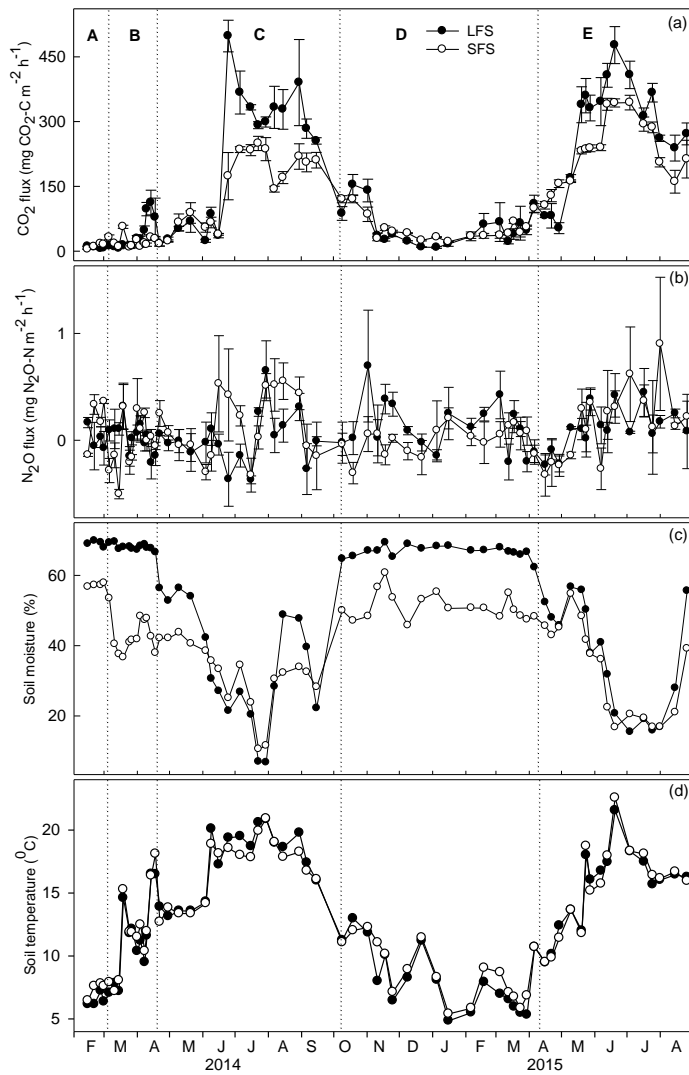


Figure 4 Variations over time in (a) CO_2 fluxes, (b) N_2O fluxes (c) soil moisture and (d) soil temperature in each site.

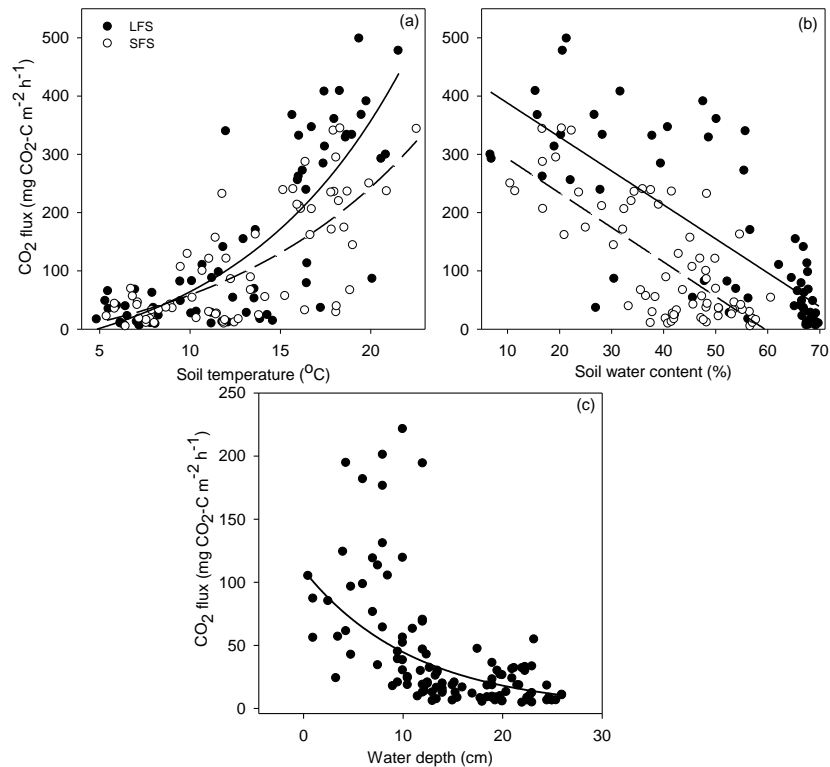


Figure 5 Relationships between CO₂ fluxes and (a) soil temperature, (b) soil moisture, and (c) water depth at individual collar position at the LFS. The lines at (a) represent the best fit regression $y = 50.69 \exp(0.09 \cdot T)$, $R^2 = 0.56$, $P < 0.001$ and $y = 53.62 \exp(0.07 \cdot T)$, $R^2 = 0.44$, $P < 0.001$ for LFS and SFS, respectively. The lines at (b) represent the best fit regression $y = 446.26 - 5.82 \cdot (\text{SWC})$, $R^2 = 0.52$, $P < 0.001$ and $y = 351.95 - 5.92 \cdot (\text{SWC})$, $R^2 = 0.54$, $P < 0.001$ for LFS and SFS, respectively. The relationship at (c) is represented by $y = 109.65 \exp(-0.04 \cdot \text{WD})$, $R^2 = 0.45$, $P < 0.001$. Values in (a) and (b) are means for $n=3-4$.

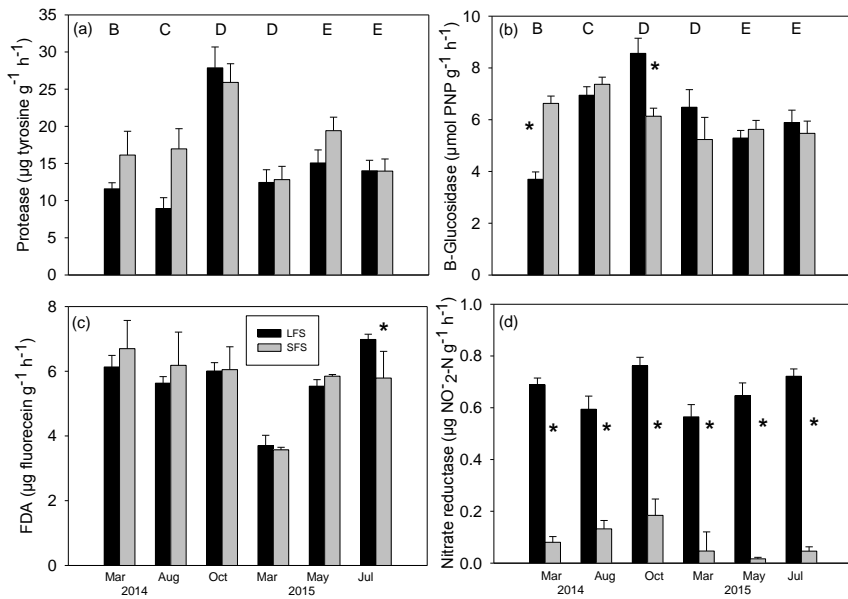


Figure 6 Soil enzymatic activities of (a) protease, (b) beta-Glucosidase, (c) fluorescein diacetate and, (d) nitrate reductase measured at different sampling dates from the LFS and SFS. The dates correspond to Periods B, C, D, E and E of Fig. 3. Values are mean \pm SE (n = 4-6). Asterisks indicate significant difference between the LFS

5 and SFS for the same sampling date at $P < 0.05$.

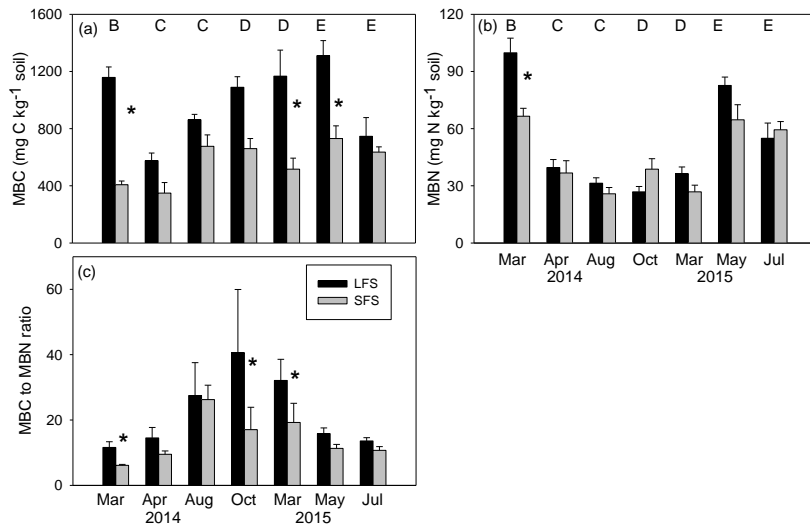


Figure 7 Seasonal variations of (a) MBC (b) MBN and (c) MBC:MBN ratio from the LFS and SFS measured at different sampling dates. The dates correspond to Period B, C, C, D, D, E and E of Fig. 3. Error bars represent the standard errors of the mean (n=4-6). Asterisks indicate significant difference between the LFS and SFS for the same sampling date at $P<0.05$.

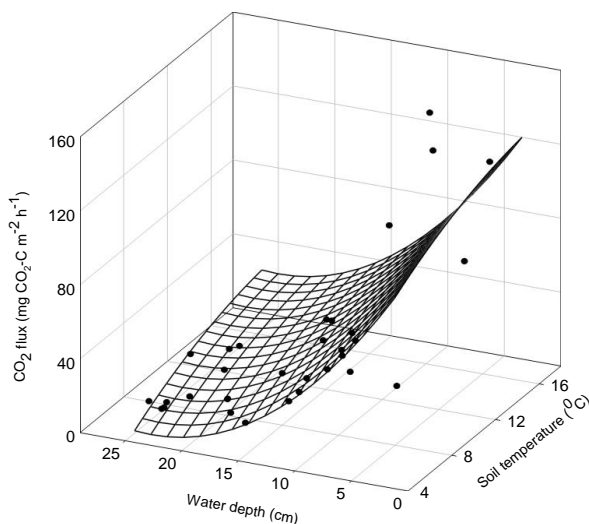


Figure 8 Dependence of CO_2 fluxes on water depth and soil temperature during the flooding period of LFS. A significant ($R^2 = 0.62$, $P < 0.001$) 3D Paraboloid regression is shown in the mesh plot. Values are mean of (n=3-4).